The Anteroventral Bed Nucleus of the Stria Terminalis Differentially Regulates Hypothalamic-Pituitary-Adrenocortical Axis Responses to Acute and Chronic Stress

Dennis C. Choi, Nathan K. Evanson, Amy R. Furay, Yvonne M. Ulrich-Lai, Michelle M. Ostrander, and James P. Herman

Neuroscience Program (D.C.C., N.K.E., A.R.F., J.P.H.), Departments of Psychiatry (D.C.C., N.K.E., A.R.F., Y.M.U.-L., M.M.O., J.P.H.) and Cell Biology, Neurobiology and Anatomy (J.P.H.), University of Cincinnati College of Medicine, Cincinnati, Ohio 45267

The anteroventral region of the bed nucleus of the stria terminalis (BST) stimulates hypothalamic-pituitary-adrenocortical (HPA) axis responses to acute stress. However, the role of the anterior BST nuclei in chronic drive of the HPA axis has yet to be established. Therefore, this study tests the role of the anteroventral BST in physiological responses to chronic drive, using a chronic variable stress (CVS) model. Male Sprague-Dawley rats received either bilateral ibotenate lesions, targeting the anteroventral BST, or vehicle injection into the same region. Half of the lesion and control rats were exposed to a 14-d CVS paradigm consisting of twice-daily exposure to unpredictable, alternating stressors. The remaining rats were nonhandled control animals that remained in home cages. On the morning after the end of CVS exposure, all rats were exposed to a novel restraint stress challenge. CVS induced attenuated body weight gain, adrenal hypertrophy, thymic involution, and enhanced CRH mRNA in hypophysiotrophic neurons of the hypothalamic paraventricular nucleus, none of which were affected by anteroventral BST lesions. In the absence of CVS, lesions attenuated the plasma corticosterone and paraventricular nucleus c-*fos* mRNA responses to the acute restraint stress. In contrast, lesions of the anteroventral BST elevated plasma ACTH and corticosterone responses to novel restraint in the rats previously exposed to CVS. These data suggest that the anterior BST plays very different roles in integrating acute stimulation and chronic drive of the HPA axis, perhaps mediated by chronic stress-induced recruitment of distinct BST cell groups or functional reorganization of stress-integrative circuits. (*Endocrinology* 149: 818–826, 2008)

ACTIVATION OF THE hypothalamic-pituitary-adrenocortical (HPA) axis is one of the primary responses to real or perceived threats (stressors). Central control of the HPA axis is localized to the paraventricular nucleus (PVN) of the hypothalamus, in which medial parvocellular hypophysiotrophic neurons synthesize CRH and arginine vasopressin (AVP). When released, CRH and AVP work synergistically to elicit secretion of ACTH from anterior pituitary corticotropes. The ACTH travels via the systemic circulation to the adrenal cortex, where it promotes synthesis and secretion of corticosteroids (*e.g.* corticosterone in the rat). Corticosteroids target numerous organ systems that are responsible for a variety of functions, including energy mobilization and cardiovascular tone. Corticosteroids also exert negative feedback control on the HPA axis itself, thereby limiting HPA activation (for review, see Ref. 1).

Prolonged stress causes numerous neuroendocrine and physiological changes that are connected to enhanced HPA axis drive, including decreased body weight gain, thymic atrophy, and adrenal hypertrophy (2–5). Chronic stress-induced physiological changes are associated with increased activation of the PVN, including elevated expression of CRH mRNA and, in some stress models, AVP mRNA (4–6). Chronic stress models typically engender elevated pre-acute stress plasma corticosterone (2, 4, 5), and can also lead to a sensitization of the HPA axis to a novel stress challenge, resulting in a facilitation of ACTH and corticosterone secretion despite an enhanced feedback signal (7–9). Excessive exposure to glucocorticoids during chronic stress is thought to be involved in numerous stress-related pathologies, including depression, posttraumatic stress disorder, and other anxiety disorders (10).

Forebrain limbic regions such as the amygdala, hippocampus, and medial prefrontal cortex are responsible for tuning HPA axis responses to stress (see Ref. 11). These limbic regions have limited to no direct innervation of the PVN (12–15) and instead use bisynaptic or multisynaptic connections through intervening structures such as the bed nucleus of the stria terminalis (BST) (12, 15). The BST receives limbic input from the amygdala, hippocampus, and prefrontal cortex (16–18), and has abundant projections to the PVN (15, 19–23). The dorsomedial (dm) and fusiform (fu) subnuclei, which are

located in the anterior division of the BST ventral to the anterior commissure, send heavy projections to the medial parvocellular PVN (20, 22). Stimulation of the anterior or lateral areas of the BST increases HPA axis activity, whereas lesions of these areas decrease stress-induced ACTH and corticosterone secretion (24–30). Combined, these data suggest that these anterior BST structures are positioned to relay stress-excitatory information to the PVN.

The contribution of the BST to chronic stress adaptation has yet to be assessed. Given the prominent role of this structure in acute stress responsiveness, it is important to determine whether this region plays a role in the development or maintenance of chronic stress symptomology. Therefore, this current study uses selective lesions targeting the PVN-projecting dm/fu nuclei to test the hypothesis that these nuclei are necessary for sensitization of HPA axis responsivity after chronic stress. To test our hypothesis, this study uses a chronic variable stress (CVS) paradigm, followed by a novel restraint challenge to assess CVS-induced adaptations in HPA axis reactivity.

Materials and Methods

Experimental animals

A total of 54 adult male Sprague-Dawley rats (275–300 g; Harlan, Indianapolis, IN) was used for this study. All rats were housed three per cage in conventional shoebox rat cages with food and water available *ad libitum* in a temperature and humidity controlled vivarium on a 12-h light, 12-h dark cycle (lights on at 0600 h). Upon arrival, all rats acclimated to the animal facility for at least 7 d before surgery. Animals were maintained in accordance with the Guide for the Care and Use of Laboratory Animals (National Institutes of Health, 1996). All animal protocols were approved by the Institutional Animal Care and Use Committee at the University of Cincinnati.

Ibotenate lesions

Rats were anesthetized by ip injection of a 87 mg/kg ketamine/13 mg/kg xylazine mixture. Preemptive analgesia was administered by sc injections of 260 μg/kg butorphanol (Torbugesic, Fort Dodge Animal Health, Fort Dodge, IA). Each rat was mounted in a Kopf stereotaxic apparatus (David Kopf Instruments, Tujunga, CA). Skulls were exposed, and burr holes were drilled at the calculated surface coordinates. Each rat received bilateral microinjections of ibotenate (0.5 μl/side, 5.0 μg/μl) in sterile PBS (pH 7.4) or 0.9% sterile saline into the anterior BST [anterior-posterior (AP) −0.10 mm, medial-lateral ±1.5 mm, dorsal-ventral (dura) −7.0 mm], with coordinates calculated from bregma (31). Each microinjection used a 26-gauge 1-μl Hamilton injection syringe (Hamilton Co., Reno, NV), mounted on the stereotaxic apparatus. Syringes were slowly lowered to the dorsal-ventral coordinate over a 1-min period and left in place for 1 min before injection. The ibotenate or saline was manually infused over 5 min at a rate of 0.05 μl/30 sec, followed by another 5-min waiting period to allow diffusion and minimize dorsal spread of injection up the needle track. The syringes were raised over a 1-min period. Skull burr holes were sealed with sterile bone wax, and the skin was closed with wound clips. Animals recovered for at least 7 d after surgery before CVS exposure. Body weights were measured on the day of surgery, d-1 CVS exposure, d-8 CVS exposure, d 15 after restraint stress challenge, and just before sacrifice.

CVS protocol

Rats were randomly assigned to "sham non-CVS" (n = 12), "sham CVS" (n = 12), "lesion non-CVS" (n = 15), and "lesion CVS" (n = 15) groups, in which "CVS" groups were exposed to the CVS paradigm, whereas "non-CVS" rats remained in their home cages as unhandled controls. The CVS paradigm consisted of twice-daily exposure to alternating stressors for 14 consecutive days (d 1–14). Morning stressors were

administered between 0930 and 1030 h, whereas afternoon stressors were conducted between 1430 and 1530 h. Occasional overnight stressors began immediately after cessation of afternoon stressors and ended with initiation of the next day's morning stressor. CVS stressors consisted of hypoxia (30 min in 8% oxygen), cold stress (1 h at 4 C, two rats per cage without bedding), rotation stress (1 h at 100 rpm on a platform orbital shaker), warm swim (20 min at 31–33 C), cold swim (10 min at 16–18 C), overnight social isolation (one rat per cage), and overnight social crowding (six rats per cage). Stressors were unpredictable for the rats by being presented in a semi-randomized order, with each stressor (except the overnight stressors) representing an equivalent number of times.

Acute novel restraint stress protocol

All rats received restraint stress between 0830 and 1030 h on d 15, the day after the cessation of CVS. Animals were placed in well-ventilated Plexiglas restraint tubes (Altuglas International, Philadelphia, PA), and a tail clip blood sample (250–300 μl) was immediately collected for the determination of plasma ACTH and corticosterone levels. All rats remained in the restrainers for 20 min, at which point another blood sample was collected. Animals were then released back into their home cages to recover. An additional blood sample was taken at 40 min from the onset of the restraint stress. At 60 min from the onset of restraint, the rats were immediately killed by decapitation, and trunk blood was collected. Brains were removed, flash frozen in isopentane on dry ice (−45 C), and stored at −80 C. Adrenal and thymus glands were also collected and weighed.

RIA

Plasma corticosterone levels were measured by RIA using a kit from MP Biomedicals (Orangeburg, NY); plasma ACTH levels were measured by RIA using an antiserum donated by Dr. W. Engeland (University of Minnesota, Minneapolis, MN) and ^{125}I-labeled ACTH (Amersham Biosciences, Piscataway, NJ) as tracer (32). For each hormone, all plasma samples were analyzed in duplicate within the same assay. Samples were randomized within assay runs. For the ACTH RIA, the intraassay coefficient of variation was 13% for plasma pools of 38 pg/ml. For the corticosterone RIA, the intraassay coefficient of variation was 8% for plasma pools of 120 ng/ml, which mirrors the manufacturer specifications.

Lesion verification

Brains were serially sectioned at 14 μm using a MICROM cryostat (MICROM International GmbH, Walldorf, Germany), mounted onto charged glass slides and stored at −20 C. Lesion sites were verified by both Nissl staining of cells and neuronal nuclei (NeuN) immunolabeling as a neuronal marker. Sections were fixed in 4% paraformaldehyde and Nissl stained with cresyl violet, dehydrated through an ascending ethanol series, cleared in xylene, and coverslipped using DPX mountant. For NeuN immunohistochemistry, tissue sections were encircled by a hydrophobic slide marker (Super HT PAP pen; Research Products International Corp., Mt. Prospect, IL). The tissue sections were fixed in 4% paraformaldehyde and washed extensively with 50 mM potassium phosphate buffered-saline (KPBS) between each step. Subsequently, sections were incubated in 1% H_2O_2 for 10 min and blocked in incubation solution (4% normal goat serum and 0.3% Triton X-100 in KPBS) for 1 h. Sections were incubated overnight with a monoclonal antibody against NeuN (1:1000; CHEMICON International, Inc., Temecula, CA) with Parafilm coverslips (American National Can Co., Greenwich, CT), followed by a 1-h incubation in biotinylated donkey antigoat IgG (1:500; Vector Laboratories, Burlingame, CA) and a 1-h incubation in avidin-horseradish peroxidase complex (1:500, ABC Elite Kit; Vector Laboratories), in which each step was in incubation solution. Finally, sections were incubated for 5 min in 0.02% diaminobenzidine (Sigma-Aldrich, St. Louis, MO), resulting in a brown reaction product. Slides were dehydrated through an ascending ethanol series, cleared in xylene, and coverslipped using DPX mountant.

Lesions were identified by the location of the needle track, loss of neurons, gliosis, and sparing damage to fibers of passage (33). Lesions targeting the anterior division of the BST were confirmed as "hits" when

the primary damage included the fu and dm nuclei of the BST, with some occasional damage extending into the adjacent subcommissural zone of the BST, the ventral pallidum, and the parastrial nucleus. Lesions that focused outside of the primary targeted dm/fu nuclei of the BST were considered misses. Rats with bilateral damage were included in the study, whereas rats with only partial unilateral lesions or missed lesions were removed from the analysis. The final "n" for experimental groups after lesion verification were: "sham non-CVS" (n = 12), "sham CVS" (n = 12), "lesion non-CVS" (n = 9), and "lesion CVS" (n = 10).

In situ hybridization

Antisense AVP, CRH, and c-*fos* riboprobes were generated by *in vitro* transcription using ^{35}S-labeled uridine 5c-triphosphate (UTP). The rat AVP (exon C) cDNA construct is a 161-bp insert in a pCR4 TOPO vector, which was linearized with NotI restriction enzyme, and transcribed using T3 RNA polymerase. The rat c-*fos* cDNA construct (courtesy of Dr. T. Curran, Children's Hospital of Philadelphia, PA) is a 587-bp fragment cloned into Bluescript SK vector, which was linearized with HindIII and transcribed with T3 RNA polymerase. The rat CRH cDNA construct is a 765-bp fragment cloned into pGEM3 vector (courtesy of Dr. Robert Thompson, University of Michigan, Ann Arbor, MI), which was linearized with HindIII and transcribed using T7 RNA polymerase. Each 15-μl riboprobe transcription reaction was made from 1.0- to 2.5-μg linearized DNA fragment, 62.5 μCi ^{35}S-UTP, 330 μM ATP, 330 μM guanosine 5c-triphosphate, 330 μM cytidine 5c-triphosphate, 10 μM cold UTP, 1× transcription buffer, 66.6 mM dithiothreitol, 40 U RNase Inhibitor, and 20 U of the appropriate RNA polymerase.

Before hybridization, tissue slides were pretreated with 4% paraformaldehyde, washed in KPBS, acetylated, delipidized in chloroform, and dehydrated through a graded ethanol series. Each riboprobe was diluted (1.0×10^6 cpm/50 μl buffer) in hybridization buffer (50% formamide, 1× Denhardt's Solution, 10% dextran sulfate, 200 μg/ml fish sperm single-stranded DNA, 100 μg/ml yeast tRNA, and 20 mM dithiothreitol), and applied to a one in 10 series of slides containing the mounted brain sections cut on the cryostat. Slides with hybridization media were then coverslipped, placed in hybridization chambers over blotting paper soaked in 50% formamide, and incubated overnight at 55 C. The next day, coverslips were removed and slides washed in 2× standard saline citrate (SSC). Slides were subsequently incubated in 100 μg/ml RNase A for 30 min at 37 C, washed numerous times in 0.2× SSC, once in 0.2× SSC for 1 h at 65 C, and finally dehydrated through a graded ethanol series.

Image analysis

Hybridized slides were exposed on Kodak Biomax MR film (Eastman Kodak Co., Rochester, NY) (5 h for AVP, 7 d for CRH, and 14 d for c-*fos*). Film images of brain sections were captured by a digital video camera. Anatomical brain regions were identified using Swanson (34), and Paxinos and Watson (31) rat brain atlases. Brain sections were matched for rostrocaudal level between rats for analyses. All brain regions and nuclei were clearly distinguishable by the specificity and intensity of AVP, CRH, and c-*fos* expression patterns. The parvocellular and magnocellular aspects of the PVN were identified using the Nissl stained sections from a parallel series of tissue as a guide. Semiquantitative analyses of autoradiograph images were performed using Scion Image (Scion, Frederick, MD) software, and hybridization signal was expressed as gray level units. The gray level signal of a hybridized tissue region of interest was corrected by subtracting the gray level signal over a nonhybridized area of tissue (white matter, corpus callosum), and expressed as corrected gray level. [14]C standards were also measured using Scion Image, and transferred to Assay Zap (Biosoft, Cambridge, UK, and P. L. Taylor) to generate a standard curve to verify that all measured gray levels were in the linear range of the film.

Statistical analysis

Data are expressed as mean ± SEM. To consider differences in body weight, adjusted thymus and adrenal gland weights were calculated as organ weight (mg) divided by final body weight (g) and multiplied by 100. AVP, CRH, and c-*fos* mRNA expression were expressed as corrected gray level. Integrated plasma ACTH and corticosterone responses were

calculated as total area under the curve (AUC) for the restraint time course. AUC was calculated using the trapezoid rule. The trapezoid area under each two adjacent hormonal data points (a and b) are calculated by (a + b)/2 t, where t = time between a and b. The total AUC is calculated by summating all the trapezoid areas under each two adjacent hormonal time points.

Organ weights, pre-acute stress plasma hormones, integrated plasma hormones, and *in situ* hybridization data were analyzed by two-way
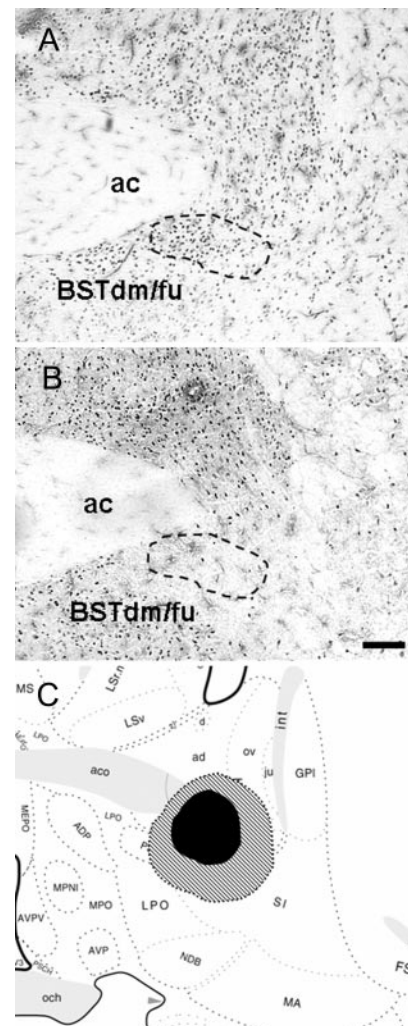

FIG. 1. Brain tissue sections were immunolabeled for NeuN for analyses of the extent of lesions of the anteroventral BST, targeting the dm and fu nuclei (BSTdm/fu) of the BST. A, Sham injection sites have intact neurons, minimal gliosis, and minimal needle track damage. B, In contrast, anteroventral BST lesions were identified by damage ventral to the anterior commissure (ac) at approximately AP −0.15 to −0.3 mm from bregma. *Scale bars*, 300 μm. C, Schematic diagram illustrates the extent of the spread of damage of the smallest (*black shaded area*) to the largest lesions (*cross-hatched shaded area*) confirmed as hits of the anteroventral BST. Image adapted from Swanson (34). aco, Anterior commissure, olfactory limb; ad, BST anterodorsal area; ADP, anterodorsal preoptic nucleus; AVP, anteroventral preoptic nucleus; AVPV, anteroventral periventricular nucleus hypothalamus; FS, fundus of the striatum; GPl, globus pallidus, lateral segment; int, internal capsule; ju, BST juxtacapsular nucleus; LPO, lateral preoptic area; LSv, lateral septal nucleus, ventral part; MA, magnocellular preoptic nucleus; MEPO, median preoptic nucleus; MPNl, medial preoptic nucleus, lateral part; MPO, medial preoptic area; MS, medial septal nucleus; NDB, nucleus of the diagonal band; och, optic chiasm; ov, BST oval nucleus; SI, substantia innominata.

TABLE 1. Body weight after anteroventral BST lesion and chronic stress

	No CVS		CVS	
	Sham	Lesion	Sham	Lesion
d −6 (Surgery) % body weight gain	100 ± 0.0	100 ± 0.0	100 ± 0.0	100 ± 0.0
d 1 CVS % body weight gain	104 ± 0.6	104 ± 1.3	106 ± 0.5	104 ± 1.0
d 8 CVS % body weight gain	112 ± 1.3	113 ± 1.9	103 ± 1.1[a]	105 ± 1.1[a]
d 15 (End of CVS) % body weight gain	120 ± 1.1	118 ± 2.3	110 ± 1.0[a]	109 ± 1.2[a]

Data are shown as mean ± SEM (n = 9–12).
[a] $P < 0.05$ *vs.* respective "No CVS."

factorial ANOVA (lesion, CVS), and significant main effects were further analyzed by Fisher's least significant difference *post hoc* test. Body weight and the time course of plasma ACTH and corticosterone responses to restraint were analyzed by three-way ANOVA (lesion, CVS, time) with repeated measures (time), and significant main effects were further analyzed by Fisher's least significant difference *post hoc* tests. Hormone and body weight data were analyzed using GBStat (Dynamic Microsystems Inc., Silver Spring, MD), whereas organ weight and mRNA data were analyzed using StatView (SAS Institute Inc., Cary, NC). Statistical significance was set at $P < 0.05$. Tests for homogeneity of variance were performed, and when necessary, log transformations were used. Detection of outliers was performed using the Dixon-Massey method, and when necessary, data were reanalyzed following outlier removal and/or transformations.

Results

Lesions of the BSTdm/fu nuclei

The role of the dm/fu nuclei of the BST in HPA axis regulation after acute and/or chronic stress exposure was assessed using bilateral ibotenate lesions targeting these nuclei. Lesion location and extent were verified by Nissl stain and NeuN immunolabeling (Fig. 1). Confirmed anterior BST lesions were centered ventral to the anterior commissure at approximately AP −0.10 mm from bregma, and were relatively consistent in the extent of damage. For all the data in this study, the bilateral lesions were confirmed as "hits" when the damage primarily included the fu and dm nuclei of the BST, with limited damage extending into the adjacent subcommissural zone. The rats with lesion damage localized outside of the targeted BST nuclei were not included in the statistical analyses. The majority of damage in the anterior BST nuclei remained ventral to the anterior commissure with minimal needle track or lesion damage dorsal to the anterior commissure, minimal ventral damage in the medial preoptic area, and no caudal damage in the posterior division of the BST.

Body and organ weights

There were main effects of CVS ($F_{1,167} = 33.25$; $P < 0.05$) and day ($F_{3,167} = 273.47$; $P < 0.05$), and interactions between CVS × day ($F_{3,167} = 64.16$; $P < 0.05$), and lesion × day ($F_{3,167} = 3.21.16$; $P < 0.05$) on body weight (Table 1). However, there was no effect of lesion on body weight gain, no lesion × day interaction, and no lesion × CVS × day interaction, indicating that destruction of the BSTdm/fu is not sufficient to alter the consequences of chronic stress on body weight.

There were main effects of CVS on raw adrenal weights (Table 2) ($F_{1,38} = 18.60$; $P < 0.05$) and adjusted adrenal weights ($F_{1,38} = 71.85$; $P < 0.05$). However, there were no

effects of lesion on raw or adjusted adrenal weights, and there was no lesion × CVS interaction. More specifically, CVS groups had greater raw and adjusted adrenal weights ($P < 0.05$) than their respective non-CVS groups, suggesting that CVS induced adrenal hypertrophy/hyperplasia regardless of lesion.

There was a main effect of CVS on raw thymus weights (Table 2) ($F_{1,38} = 9.73$; $P < 0.05$), but no effect of CVS on thymus weight adjusted for body weight. In addition, there were no effects of lesion on raw or adjusted thymus weights, and there was no lesion × CVS interaction. Overall, the data indicate that CVS decreases thymic weight to the same extent in lesion and control animals.

Pre-acute stress plasma ACTH levels

For pre-acute stress morning plasma ACTH (Fig. 2A), there was a main effect of CVS ($F_{1,37} = 15.46$; $P < 0.05$) and lesion ($F_{1,37} = 7.03$; $P < 0.05$). *Post hoc* analyses revealed that CVS exposure elevated pre-acute stress plasma ACTH levels only in rats with BST lesions.

Plasma ACTH responses to novel stress

Time-course analysis of ACTH responses to restraint (Fig. 2, B and C) indicated main effects of time ($F_{3,163} = 52.26$; $P < 0.05$) and CVS ($F_{1,163} = 10.04$; $P < 0.05$), and a significant CVS × time interaction ($F_{3,163} = 5.77$; $P < 0.05$). However, there was no main effect of lesion on ACTH secretion, and there were no other interactions. *Post hoc* analyses indicated that in CVS rats, lesions augmented plasma ACTH levels at 20 min after the onset of restraint ($P < 0.05$). There was also a main effect of CVS on integrated plasma ACTH response to restraint (Fig. 2D) ($F_{1,36} = 10.33$; $P < 0.05$), but no effect of lesion, and no lesion × CVS interaction. *Post hoc* analyses revealed that CVS elevated the integrated ACTH levels only in rats with lesions ($P < 0.05$).

Pre-acute stress plasma corticosterone levels

There was a main effect of CVS on pre-acute stress AM plasma corticosterone levels (Fig. 3A) ($F_{1,38} = 27.22$; $P < 0.05$), but no effect of lesion, and no lesion × CVS interaction. *Post hoc* analyses indicated that CVS exposure increased pre-acute stress corticosterone levels regardless of lesion ($P < 0.05$). These data indicate that chronic stress increases resting corticosterone levels to an equal extent in lesion and control groups.

TABLE 2. Adrenal and thymus weight after anteroventral BST lesion and chronic stress

	No CVS		CVS	
	Sham	Lesion	Sham	Lesion
Raw adrenal (mg)	51.2 ± 1.2	49.6 ± 1.0	56.9 ± 1.2^a	56.6 ± 2.2^a
Adjusted adrenal (mg/100 g BW)	13.8 ± 0.3	13.6 ± 0.4	17.2 ± 0.3^a	17.3 ± 0.6^a
Raw thymus (mg)	363 ± 17	375 ± 31	314 ± 13^a	301 ± 17^a
Adjusted thymus (mg/100g BW)	98 ± 5.1	102 ± 7.1	96 ± 4.3	92 ± 4.6

Data are shown as mean $\pm$ SEM (n = 9–12). BW, Body weight.
[a] $P < 0.05$ *vs.* respective "No CVS."

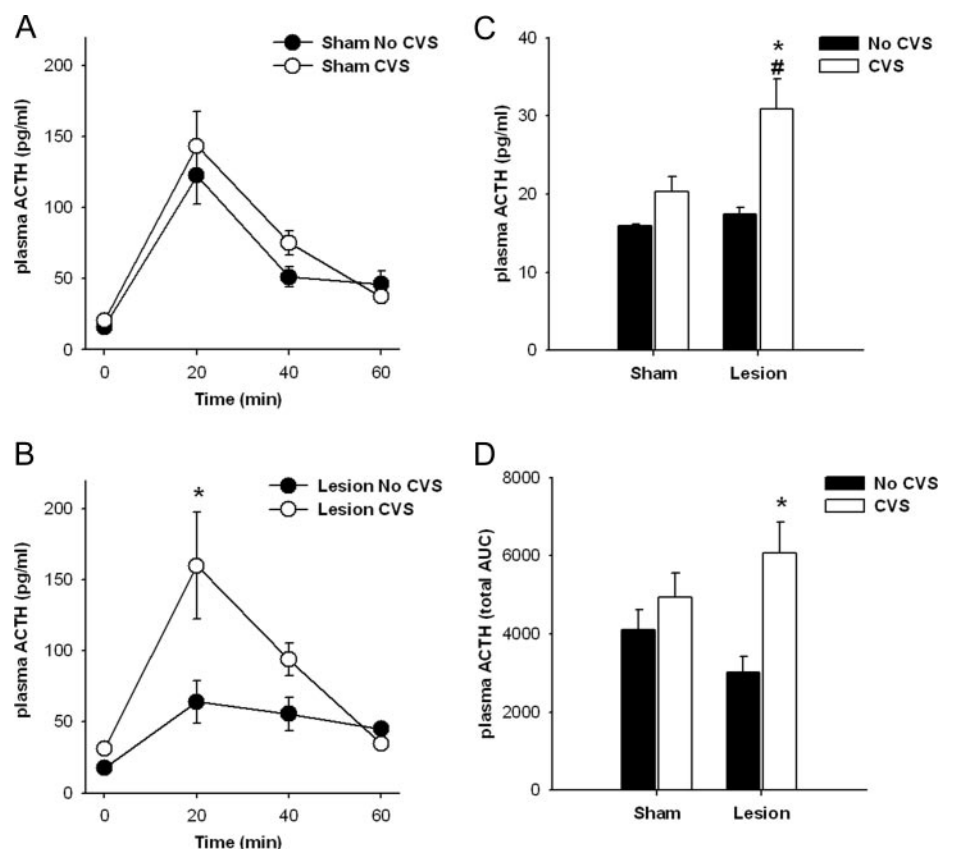*Plasma corticosterone responses to novel stress*

There was a significant effect of CVS ($F_{1,167} = 24.23$; $P < 0.05$) and time ($F_{3,167} = 196.30$; $P < 0.05$) on the plasma corticosterone response to a 20-min novel restraint (Fig. 3, B and C), but no main effect of lesion. However, both lesion × time ($F_{3,167} = 4.98$; $P < 0.05$) and lesion × CVS ($F_{3,167} = 5.75$; $P < 0.05$) interactions were significant, indicative of differential effects of lesions on corticosterone secretion. *Post hoc* analyses revealed that in rats with lesions, prior CVS exposure elevated plasma corticosterone levels at 20 ($P < 0.05$), 40 ($P < 0.05$), and 60 min ($P < 0.05$) after the onset of restraint relative to rats with lesions and no prior exposure to CVS. In addition, in animals with no prior exposure to CVS, lesions significantly decreased plasma corticosterone response at 60 min after the onset of restraint ($P < 0.05$). There was also a main effect of CVS on integrated plasma corticosterone response to restraint (Fig. 3D) ($F_{1,38} = 15.75$; $P < 0.05$), but there was no effect of lesion, and no lesion × CVS interaction. *Post hoc* anal-

yses indicated that in rats with lesions, prior CVS exposure elevated the integrated corticosterone levels ($P < 0.05$). Together, these data are consistent with previous lesion studies indicating an excitatory role for the anterior BST in acute stress excitation (30) but suggest that this region plays a role in inhibition of acute stress responses after prolonged stress.

c-fos mRNA expression in the PVN

Induction of a PVN c-*fos* mRNA response to novel restraint stress was assessed as an indirect indicator of neuronal activation (Fig. 4). There was a main effect of lesion on c-*fos* mRNA in the PVN ($F_{1,37} = 5.94$; $P < 0.05$), but no effect of CVS, and there was no lesion × CVS interaction. *Post hoc* analysis revealed that in the rats with no prior exposure to CVS, lesions reduced PVN c-*fos* mRNA expression ($P < 0.05$), as previously documented (30).

FIG. 2. A, In sham rats, prior CVS exposure did not affect the plasma ACTH response to 20-min restraint stress. B, In rats with lesions, prior CVS exposure elevated the plasma ACTH response to an acute 20-min restraint at the 20-min time point compared with rats with lesions and no prior exposure to CVS. C, In rats with lesions, CVS significantly elevated pre-acute stress AM plasma ACTH levels. Anteroventral BST lesions potentiated pre-acute stress AM plasma ACTH levels only in the rats exposed to CVS. D, In rats with prior exposure to CVS, anteroventral BST lesions elevated the integrated ACTH response. Data are presented as mean $\pm$ SEM (n = 9–12). *, $P < 0.05$ *vs.* respective "No CVS." #, $P < 0.05$ *vs.* respective Sham.
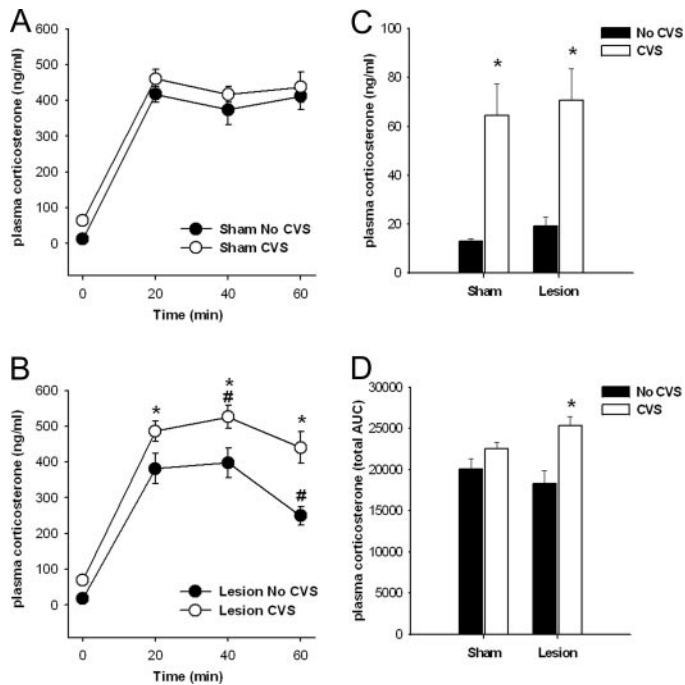
FIG. 3. A, In sham rats, prior CVS exposure did not affect the plasma corticosterone response to 20-min restraint stress. A and B, In rats with no prior exposure to CVS, lesions attenuated the plasma corticosterone levels at the 60-min time point relative to all other groups. B, In rats with lesions, CVS elevated plasma corticosterone responses to restraint at the 20-, 40-, and 60-min time points relative to the lesion-no CVS group. Lesions also increased post-CVS plasma corticosterone responses relative to the CVS, nonlesion groups. C, Pre-acute stress AM plasma corticosterone levels were elevated by CVS exposure but were not affected by lesions of the anteroventral BST. D, In rats with lesions, CVS elevated the integrated plasma corticosterone response. Data are presented as mean ± SEM (n = 9–12). *, $P < 0.05$ *vs.* respective "No CVS." #, $P < 0.05$ *vs.* respective sham (panel B *vs.* A).
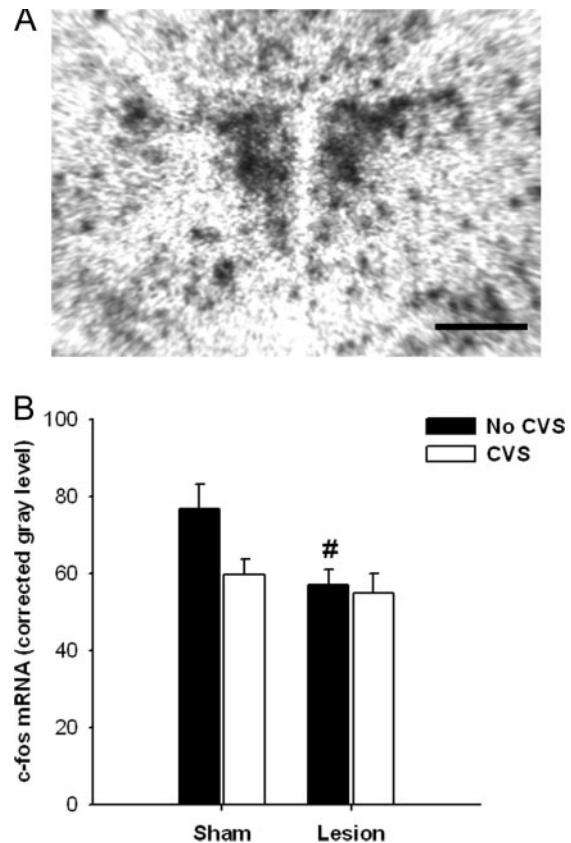

FIG. 4. A, Representative image of c-*fos* mRNA expression in the PVN of the hypothalamus as assessed by *in situ* hybridization. B, Semiquantitative analysis revealed that PVN c-*fos* mRNA expression was attenuated by anteroventral BST lesions in "No CVS" rats compared with respective sham rats. Data are shown as mean ± SEM (n = 9–12). #, $P < 0.05$ *vs.* respective sham. *Scale bar*, 500 μm.

CRH and vasopressin mRNA expression in the PVN

CRH mRNA expression in the PVN (Fig. 5) and AVP mRNA expression in the medial parvocellular aspect of the PVN (Fig. 6) were assessed as indicators of central HPA axis tone. There was a significant effect of CVS on CRH mRNA in the PVN ($F_{1,37} = 14.13$; $P < 0.05$), but there was no effect of lesion, and there was no lesion × CVS interaction. *Post hoc* analyses revealed that CVS significantly elevated CRH mRNA expression in the PVN regardless of lesion ($P < 0.05$).

There were no significant effects of lesion or CVS on AVP mRNA expression in the parvocellular PVN, and there was no lesion × CVS interaction. Similarly, there were no differences among experimental groups for magnocellular AVP expression in the posterior magnocellular PVN or in the supraoptic nucleus (data not shown).

Discussion

The current study demonstrates that damage to the anteroventral BST, encompassing the PVN-projecting BSTdm/fu subnuclei, has divergent effects on HPA axis responses to acute *vs.* chronic stress. Anteroventral BST lesions reduced c-*fos* activation of the PVN and corticosterone secretion in response to acute restraint, whereas corticosterone responses to novel restraint were potentiated in rats with lesions that had prior CVS exposure. Similarly, pre-acute stress plasma ACTH, integrated ACTH, and corticosterone responses were elevated only in the CVS-exposed rats with anteroventral BST damage. Overall, the data suggest that the BSTdm/fu act as activators of the HPA axis response to acute stress challenges but are also involved in inhibitory regulation of HPA axis reactivity after chronic stress. The data are consistent with a chronic stress-induced functional reassignment of the anterior BST-PVN circuitry, occurring at or above the level of the BST.

This study used a 2-wk exposure to chronic unpredictable stress that elicited consistent physiological and neuroendocrine adaptations. CVS evoked decreased body weight gain, adrenal hypertrophy/hyperplasia, thymic involution, elevated AM resting plasma corticosterone levels, and potentiated CRH mRNA in the PVN as previously shown by our group (9, 35), suggestive of increased HPA tone. None of these endpoints was significantly affected by anterior BST lesions, suggesting that damage to this region does not alter
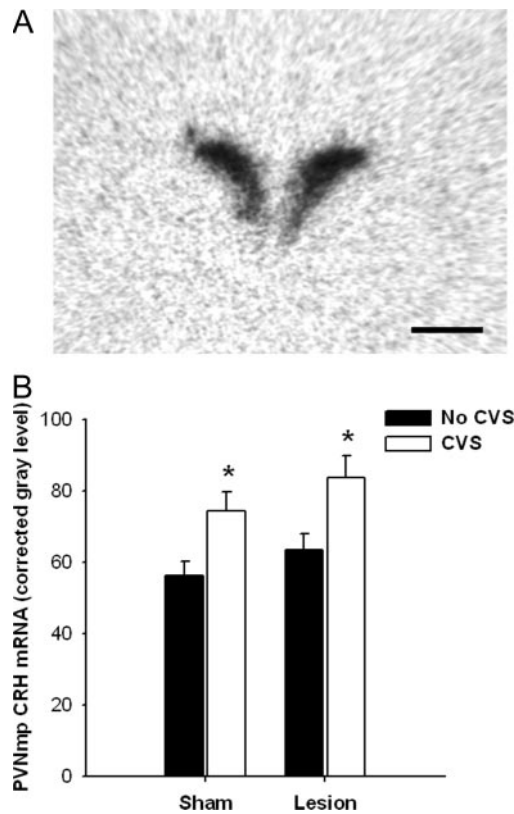
FIG. 5. A, Representative image of CRH mRNA expression in the PVN by *in situ* hybridization. B, Semiquantitative analysis revealed that PVN CRH mRNA expression was elevated by CVS exposure regardless of lesion. Data are shown as mean ± SEM (n = 9–12). *, $P <$ 0.05 *vs.* respective "No CVS." *Scale bar*, 500 μm.
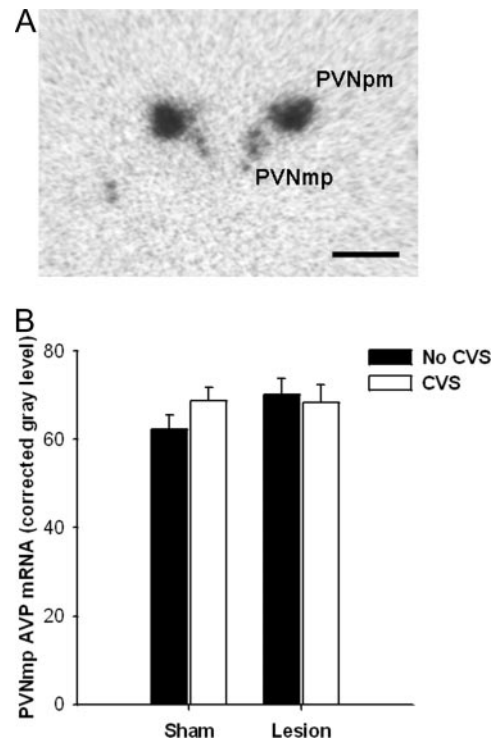

FIG. 6. A, Representative image of AVP mRNA expression in the PVN by *in situ* hybridization. B, Semiquantitative analyses revealed that PVN AVP mRNA expression was not affected by CVS exposure or lesions of the BSTdm/fu. Data are shown as mean ± SEM (n = 9–12). *Scale bar*, 500 μm. PVNmp, Medial parvocellular PVN; PVNpm, posterior magnocellular PVN.

the development of the major physiological indices of chronic stress.

The novel acute restraint challenge evoked a significant increase in plasma ACTH levels at 20 min in all groups. Moreover, this response to the restraint was further potentiated by prior CVS exposure only in rats with anteroventral BST lesions, indicating damage to a circuit that would have otherwise constrained the response. Notably, this increase can be attributed at least in part to the markedly lower ACTH response observed in rats with lesions and no prior exposure to CVS, compared with sham rats with no prior exposure to CVS. When analyzing the integrated ACTH response, the AUC was also significantly elevated by CVS only in rats with lesions, suggesting that the anteroventral BST inhibits CVS-induced sensitization of ACTH secretion. In addition, resting AM plasma ACTH levels were also augmented only in the CVS-exposed rats with lesions, suggesting enhanced pre-acute stress activation at the level of the pituitary. Overall, contrary to our *a priori* hypothesis, the dm and fu nuclei provide inhibitory drive on HPA activity after chronic stress exposure, acting to inhibit both resting AM plasma ACTH secretion and ACTH responses to stress, in contrast to a role in excitation of the HPA axis to an acute response without prior CVS exposure.

In the present work, the corticosterone response to novel restraint was significantly diminished at 60 min by an-

teroventral BST lesions in rats with no prior exposure to CVS exposure. This replicates our previous findings indicating that the anteroventral BST stimulates HPA reactivity to an acute stress (30). However, in CVS-exposed rats, lesions of the anteroventral BST potentiated the plasma corticosterone response at 40 min after onset of restraint. CVS also elevated the total integrated plasma corticosterone response and corticosterone levels at 20, 40, and 60 min after novel restraint, but only in rats with lesions of the anteroventral BST. Interestingly, we failed to see a sensitization of the corticosterone response in CVS sham rats, although this is not always observed after CVS or other chronic stress paradigms (9, 36). These data are consistent with the ACTH data and, together, indicate that the anteroventral BST clearly has opposing roles in stress responsivity, likely providing excitation during an acute stress challenge but driving inhibition after adaptations to chronic stress exposure.

At the level of the PVN, c-*fos* mRNA expression was decreased by lesions of the anteroventral BST in the absence of CVS exposure, further indicating the BSTdm/fu provides activation of the PVN in response to a single acute stressor, consistent with our previous findings (30). In contrast, the lesion-induced decrease in c-*fos* induction was not observed in rats exposed to CVS. Although there was no main effect of CVS on c-*fos* mRNA, there was a trend for CVS to decrease c-*fos* mRNA in the PVN ($P = 0.065$), similar to previous studies in our group that have reported CVS-induced de-

creases in c-*fos* mRNA in the PVN at 60 min after onset of restraint stress (9, 35). Overall, we interpret these data to suggest that a prior history of chronic stress potentially reverses the lesion-induced decrease in PVN activation and may be related to the CVS-induced up-regulated hormonal responses to restraint by CVS exposure in rats with lesions only.

In this study other indices of chronic stress were measured after CVS, including increased adrenal weight, suggestive of a history of elevated ACTH exposure (3), and thymic involution, suggestive of a history of increased circulating glucocorticoids. In addition, a rapid decline in body weight gain was observed after onset of CVS, as shown by others (37). Chronic stress is also known to up-regulate CRH and AVP in paraventricular hypophysiotrophs (4, 38, 39). We observed CVS-induced increases in CRH mRNA but not AVP mRNA expression in the PVN. However, none of these physiological or neuroendocrine adaptations to chronic stress was affected by lesions of the anteroventral BST, suggesting that disruption of these BST nuclei does not affect the development of steady-state changes in HPA function engendered by chronic stress.

There are several possible, and perhaps overlapping, mechanisms that may explain the ability of anteroventral BST lesions to inhibit acute responses in chronic stress-naive rats but potentiate responses in chronic stress-experienced animals. First, acute *vs.* chronic stress may recruit different populations of BSTdm and/or BSTfu neurons. The BSTdm/fu contains neurons using a variety of different neurotransmitters known to regulate HPA activity, including CRH, glutamate, and γ-aminobutyric acid, that are contained in distinct subpopulations (40, 41). Therefore, it is also possible that the CVS-induced switch in directionality of HPA responses may be related to destruction of separate populations of neurons that are differentially responsive to prior stress experience. Thus, excitation may prevail the first time a stressful stimulus is encountered, but additional, inhibitory neurons may be recruited upon multiple stress exposures.

Second, the BSTdm/fu receives heavy inputs from many other known stress-regulatory sites, including abundant noradrenergic inputs from the brainstem (40, 42) and limbic input from the central nucleus of the amygdala and the infralimbic cortex (12, 18). It is yet to be determined whether specific circuits from different brainstem and limbic regions converge on the same type of HPA-projecting neurons, but the dissociation between chronic and acute stress regulation by the BSTdm/fu nuclei suggests that there may be separate pools of neurons within these upstream nuclei that provide very different information or feedback about stressful stimuli.

Finally, it is possible that removal of BSTdm/fu can elicit downstream neuroplastic changes favoring PVN excitation. Thus, loss of BSTdm/fu input to the PVN or PVN-projecting structures (such as the nucleus of the solitary tract) may permit a compensatory enhancement of inputs that are preferentially sensitive to the effects of chronic stress.

In conclusion, the current study documents that the dm/fu nuclei of the BST differentially regulate HPA responses by activating acute stress responses while attenuating HPA responses after chronic unpredictable stress adaptations. We infer that the anteroventral BST contains heterogeneous populations of neurons that differentially regulate the capacity or efficiency of HPA activation, dependent on prior experience. Given that lesions of this region do not affect steady-state changes in HPA function after stress, it is likely that the anteroventral BST is involved in stress plasticity. Inappropriate limbic processing of stressful information is implicated in numerous chronic stress-related disease states (43, 44) and may involve functional changes in circuitry funneling through these important integrative BST nuclei.

References

1. **Herman JP, Figueiredo H, Mueller NK, Ulrich-Lai Y, Ostrander MM, Choi DC, Cullinan WE** 2003 Central mechanisms of stress integration: hierarchical circuitry controlling hypothalamo-pituitary-adrenocortical responsiveness. Front Neuroendocrinol 24:151–180
2. **Hauger RL, Millan MA, Lorang M, Harwood JP, Aguilera G** 1988 Corticotropin-releasing factor receptors and pituitary adrenal responses during immobilization stress. Endocrinology 123:396–405
3. **Ulrich-Lai YM, Figueiredo HF, Ostrander MM, Choi DC, Engeland WC, Herman J** 2006 Chronic stress induces adrenal hyperplasia and hypertrophy in a subregion-specific manner. Am J Physiol Endocrinol Metab 291:E965–E973
4. **Herman JP, Adams D, Prewitt C** 1995 Regulatory changes in neuroendocrine stress-integrative circuitry produced by a variable stress paradigm. Neuroendocrinology 61:180–190
5. **Kiss A, Aguilera G** 1993 Regulation of the hypothalamic pituitary adrenal axis during chronic stress: responses to repeated intraperitoneal hypertonic saline injection. Brain Res 630:262–270
6. **Imaki T, Nahan JL, Rivier C, Sawchenko PE, Vale W** 1991 Differential regulation of corticotropin-releasing factor mRNA in rat brain regions by glucocorticoids and stress. J Neurosci 11:585–599
7. **Hauger RL, Lorang M, Irwin M, Aguilera G** 1990 CRF receptor regulation and sensitization of ACTH responses to acute ether stress during chronic intermittent immobilization stress. Brain Res 532:34–40
8. **Dallman MF, Akana SF, Scribner KA, Bradbury MJ, Walker CD, Strack AM, Cascio CS** 1992 Stress, feedback and facilitation in the hypothalamo-pituitary-adrenal axis. J Neuroendocrinol 4:517–526
9. **Ostrander MM, Ulrich-Lai YM, Choi DC, Richtand NM, Herman JP** 2006 Hypoactivity of the hypothalamo-pituitary-adrenocortical axis during recovery from chronic variable stress. Endocrinology 147:2008–20017
10. **McEwen BS, Stellar E** 1993 Stress and the individual. Mechanisms leading to disease. Arch Intern Med 153:2093–2101
11. **Herman JP, Ostrander MM, Mueller NK, Figueiredo H** 2005 Limbic system mechanisms of stress regulation: hypothalamo-pituitary-adrenocortical axis. Prog Neuropsychopharmacol Biol Psychiatry 29:1201–1213
12. **Prewitt CM, Herman JP** 1998 Anatomical interactions between the central amygdaloid nucleus and the hypothalamic paraventricular nucleus of the rat: a dual tract-tracing analysis. J Chem Neuroanat 15:173–185
13. **Sawchenko PE, Swanson LW, Steinbusch HW, Verhofstad AA** 1983 The distribution and cells of origin of serotonergic inputs to the paraventricular and supraoptic nuclei of the rat. Brain Res 277:355–360
14. **Gray TS, Carney ME, Magnuson DJ** 1989 Direct projections from the central amygdaloid nucleus to the hypothalamic paraventricular nucleus: possible

role in stress-induced adrenocorticotropin release. Neuroendocrinology 50:433–446

15. **Cullinan WE, Herman JP, Watson SJ** 1993 Ventral subicular interaction with the hypothalamic paraventricular nucleus: evidence for a relay in the bed nucleus of the stria terminalis. J Comp Neurol 332:1–20
16. **Dong HW, Petrovich GD, Swanson LW** 2001 Topography of projections from amygdala to bed nuclei of the stria terminalis. Brain Res Brain Res Rev 38:192–246
17. **Canteras NS, Swanson LW** 1992 Projections of the ventral subiculum to the amygdala, septum, and hypothalamus: a PHAL anterograde tract-tracing study in the rat. J Comp Neurol 324:180–194
18. **Vertes RP** 2004 Differential projections of the infralimbic and prelimbic cortex in the rat. Synapse 51:32–58
19. **Sawchenko PE, Swanson LW** 1983 The organization of forebrain afferents to the paraventricular and supraoptic nuclei of the rat. J Comp Neurol 218:121–144
20. **Dong HW, Petrovich GD, Watts AG, Swanson LW** 2001 Basic organization of projections from the oval and fusiform nuclei of the bed nuclei of the stria terminalis in adult rat brain. J Comp Neurol 436:430–455
21. **Gu G, Cornea A, Simerly RB** 2003 Sexual differentiation of projections from the principal nucleus of the bed nuclei of the stria terminalis. J Comp Neurol 460:542–562
22. **Dong HW, Swanson LW** 2006 Projections from bed nuclei of the stria terminalis, dorsomedial nucleus: implications for cerebral hemisphere integration of neuroendocrine, autonomic, and drinking responses. J Comp Neurol 494:75–107
23. **Dong HW, Swanson LW** 2004 Projections from bed nuclei of the stria terminalis, posterior division: implications for cerebral hemisphere regulation of defensive and reproductive behaviors. J Comp Neurol 471:396–433
24. **Feldman S, Conforti N, Saphier D** 1990 The preoptic area and bed nucleus of the stria terminalis are involved in the effects of the amygdala on adrenocortical secretion. Neuroscience 37:775–779
25. **Dunn JD** 1987 Plasma corticosterone responses to electrical stimulation of the bed nucleus of the stria terminalis. Brain Res 407:327–331
26. **Zhu W, Umegaki H, Suzuki Y, Miura H, Iguchi A** 2001 Involvement of the bed nucleus of the stria terminalis in hippocampal cholinergic system-mediated activation of the hypothalamo-pituitary-adrenocortical axis in rats. Brain Res 916:101–106
27. **Casada JH, Dafny N** 1991 Restraint and stimulation of the bed nucleus of the stria terminalis produce similar stress-like behaviors. Brain Res Bull 27:207–212
28. **Herman JP, Cullinan WE, Watson SJ** 1994 Involvement of the bed nucleus of the stria terminalis in tonic regulation of paraventricular hypothalamic CRH and AVP mRNA expression. J Neuroendocrinol 6:433–442
29. **Crane JW, Buller KM, Day TA** 2003 Evidence that the bed nucleus of the stria terminalis contributes to the modulation of hypophysiotropic corticotropin-releasing factor cell responses to systemic interleukin-1β. J Comp Neurol 467:232–242

30. **Choi DC, Furay AR, Evanson NK, Ostrander MM, Ulrich-Lai YM, Herman JP** 2007 Bed nucleus of the stria terminalis subregions differentially regulate hypothalamic-pituitary-adrenal axis activity: implications for the integration of limbic inputs. J Neurosci 27:2025–2034
31. **Paxinos G, Watson C** 1998 The rat brain in stereotaxic coordinates. 4th ed. San Diego: Academic Press
32. **Jasper MS, Engeland WC** 1991 Synchronous ultradian rhythms in adrenocortical secretion detected by microdialysis in awake rats. Am J Physiol 261(5 Pt 2):R1257–R1268
33. **Herman JP, Wiegand SJ** 1986 Ibotenate-induced cell death in the hypothalamic paraventricular nucleus: differential susceptibility of magnocellular and parvicellular neurons. Brain Res 383:367–372
34. **Swanson LW** 1998 Brain maps: structure of the rat brain. 2nd ed. Amsterdam: Elsevier
35. **Ulrich-Lai YM, Ostrander MM, Thomas IM, Packard BA, Furay AR, Dolgas CM, Van Hooren DC, Figueiredo HF, Mueller NK, Choi DC, Herman JP** 2007 Daily limited access to sweetened drink attenuates hypothalamic-pituitary-adrenocortical axis stress responses. Endocrinology 148:1823–1834
36. **Choi DC, Nguyen MM, Tamashiro KL, Ma LY, Sakai RR, Herman JP** 2006 Chronic social stress in the visible burrow system modulates stress-related gene expression in the bed nucleus of the stria terminalis. Physiol Behav 89:301–310
37. **Marti O, Marti J, Armario A** 1994 Effects of chronic stress on food intake in rats: influence of stressor intensity and duration of daily exposure. Physiol Behav 55:747–753
38. **Bhatnagar S, Meaney MJ** 1995 Hypothalamic-pituitary-adrenal function in chronic intermittently cold-stressed neonatally handled and non handled rats. J Neuroendocrinol 7:97–108
39. **Makino S, Schulkin J, Smith MA, Pacak K, Palkovits M, Gold PW** 1995 Regulation of corticotropin-releasing hormone receptor messenger ribonucleic acid in the rat brain and pituitary by glucocorticoids and stress. Endocrinology 136:4517–4525
40. **Forray MI, Gysling K** 2004 Role of noradrenergic projections to the bed nucleus of the stria terminalis in the regulation of the hypothalamic-pituitary-adrenal axis. Brain Res Brain Res Rev 47:145–160
41. **Bowers G, Cullinan WE, Herman JP** 1998 Region-specific regulation of glutamic acid decarboxylase (GAD) mRNA expression in central stress circuits. J Neurosci 18:5938–5947
42. **Banihashemi L, Rinaman L** 2006 Noradrenergic inputs to the bed nucleus of the stria terminalis and paraventricular nucleus of the hypothalamus underlie hypothalamic-pituitary-adrenal axis but not hypophagic or conditioned avoidance responses to systemic yohimbine. J Neurosci 26:11442–1153
43. **McEwen BS** 1998 Stress, adaptation, and disease. Allostasis and allostatic load. Ann NY Acad Sci 840:33–44
44. **Kasckow JW, Baker D, Geracioti Jr TD** 2001 Corticotropin-releasing hormone in depression and post-traumatic stress disorder. Peptides 22:845–851

Endocrinology **is published monthly by The Endocrine Society (http://www.endo-society.org), the foremost professional society serving the endocrine community.**